Structural Engineering and Mechanics, Vol. 8, No. 4 (1999) 325-341
DOI: http://dx.doi.org/10.12989/sem.1999.8.4.325

Limit analysis of plates-a finite element formulation*

Antonio Capsoni† and Leone Corradi‡

Department of Structural Engineering, Politecnico di Milano, Piazza Leonardo da Vinci 32, 20133 Milano, Italy

Abstract. A procedure for the computation of the load carrying capacity of perfectly plastic plates in bending is presented. The approach, based on the kinematic theorem of limit analysis, requires the evaluation of the minimum of a convex, but non-smooth, function under linear equality constraints. A systematic solution procedure is devised, which detects and eliminates the finite elements which are predicted as rigid in the collapse mechanism, thus reducing the problem to the search for the minimum of a smooth and essentially unconstrained function of nodal velocities. Both Kirchhoff and Mindlin plate models are considered. The effectiveness of the approach is illustrated by means of some examples.

Key words: rigid-plastic material; limit analysis; plates.

1. Introduction

Limit analysis is the branch of plasticity which predicts the load bearing capacity of ductile structures without resorting to evolutive elastic plastic computations. The interest in developing efficient numerical solution strategies based on finite element models is well witnessed by the continuous growing of papers on the subject (e.g., Yang 1988, Liu *et al.* 1995, Sloan and Kleeman 1995, Jiang 1995, Ponter and Carter 1997).

A procedure for the finite element computation of the limit load of perfectly plastic plates composed by von Mises' material is presented. The kinematic (upper bound) theorem of limit analysis is exploited, requiring the computation of the minimum of the dissipation power associated to any possible mechanisms, after their amplitude has been normalized by imposing that the power of basic loads be unitary. In contrast to some previous proposals (Bottero *et al.* 1980, Casciaro and Cascini 1982, Christiansen and Larsen 1983, for earlier results see Cohn and Maier 1979), the present approach does not involve inequality constraints and reduces the problem to the search of the free minimum of a convex, albeit not everywhere differentiable, functional which, after finite element discretization, becomes a function of nodal velocities.

As such, the formulation does not entail significant novelties (actually, for Kirchhoff plates it

*Partial results were presented at the COMPLAS 5 Conference (Barcelona, March 1997) and at the 13th AIMETA Congress (Siena, October 1997)
† Assistant Professor
‡ Professor

was already used thirty years ago, see Hodge and Belytschko 1968). A distinctive feature of the present approach rests on the solution procedure adopted. Owing to the nature of the dissipation power, the objective function is not differentiable in the regions of the plate which keep rigid in a mechanism. By exploiting the *natural formulation* (Argyris 1966), a method is devised for detecting and eliminating from the problem the finite elements which are rigid in the final mechanism. When this has been identified, the system consists of plastically deforming elements only. As a consequence, the objective function is everywhere differentiable and the optimum is identified by a stationary condition.

The procedure, proposed in Capsoni and Corradi (1997) and successfully applied to perfectly plastic solids in plane strain, is reconsidered here for plates in bending. Both Kirchhoff and Mindlin models are examined and the relevant finite element discretizations established. For Kirchhoff plates, a fully compatible (C^1 continuous) element is used. In the Mindlin based approach compatibility would induce locking at the thin plate limit, which is encompassed by means of a mixed (assumed strain) formulation, established so that the kinematic (upper bound) nature of the model is not jeopardized. The effectiveness of the approach is demonstrated by solving a number of rectangular plates with different boundary and loading conditions. When, with increasing mesh refinement, convergence is attained in both cases, results for Kirchhoff and thin Mindlin plates differ by a negligible amount only, suggesting that the correct collapse load was maybe identified.

A side result of this study refers to the yield condition for Mindlin solid plates. The one most commonly used is an extension of that introduced by Hodge (1959) for ideal I-beams and is preferred because of its simplicity. The present approach allows for (numerically) integrating the dissipation power over the plate thickness, thus producing in an extremely simple manner the value associated to the yield condition equivalent to Hodge's result for rectangular cross sections. An example referring to a Timoshenko beam indicates that differences, even if not dramatic, may be of engineering significance.

2. Basic relations

Consider a rigid-perfectly plastic plate, identified by its middle plane Ω of boundary $\partial\Omega$ and its thickness $h(x, y)$ and acted upon by a middle plane pressure and surface loads on the free portion $\partial\Omega_\sigma$ of its boundary. The constrained boundary $\partial\Omega_u$ is fixed. According to Mindlin's hypotheses, if w and $\boldsymbol{\theta}$ denote the transverse displacement and the rotation vector, the strain field is expressed by the relations

$$\boldsymbol{\varepsilon} = z\,\boldsymbol{\kappa} \qquad \boldsymbol{\kappa} = -\nabla_s \boldsymbol{\theta} \tag{1a, b}$$

$$\boldsymbol{\gamma} = \nabla w - \boldsymbol{\theta} \tag{2}$$

where $\boldsymbol{\varepsilon}$ and $\boldsymbol{\kappa}$ are the membrane strain and the curvature tensors, respectively and $\boldsymbol{\gamma}$ is the transverse shear strain vector. The symbol $\nabla(\ )$ indicates the gradient operator and $\nabla_s(\ )$ its symmetric part.

The material being perfectly plastic, membrane stresses $\boldsymbol{\sigma}$ and transverse shears $\boldsymbol{\tau}$ are confined within the convex domain $\varphi(\boldsymbol{\sigma}, \boldsymbol{\tau}) \leq 0$, $\varphi(\boldsymbol{\sigma}, \boldsymbol{\tau})$ being the *yield function*. If von Mises' criterion is adopted, one has

$$\varphi(\boldsymbol{\sigma}, \boldsymbol{\tau}) = \sqrt{(\boldsymbol{\sigma}^t \boldsymbol{P}_m \boldsymbol{\sigma} + \boldsymbol{\tau}^t \boldsymbol{P}_s \boldsymbol{\tau})} - \sigma_0 \tag{3a}$$

where

$$\boldsymbol{P}_m = \frac{1}{2}\begin{bmatrix} 2 & -1 & 0 \\ -1 & 2 & 0 \\ 0 & 0 & 6 \end{bmatrix} \qquad \boldsymbol{P}_s = \begin{bmatrix} 3 & 0 \\ 0 & 3 \end{bmatrix} \tag{3b, c}$$

and σ_0 is the tensile yield stress. Deformations in the plate can only consist of plastic contributions, governed by the flow rule

$$\dot{\boldsymbol{\varepsilon}} = \frac{\partial \varphi}{\partial \boldsymbol{\sigma}} \dot{\lambda}, \qquad \dot{\boldsymbol{\gamma}} = \frac{\partial \varphi}{\partial \boldsymbol{\tau}} \dot{\lambda}, \qquad \dot{\lambda} \geq 0 \tag{4}$$

Eqs. (4) act as a kinematic constraint which confines the admissible strain rates in the subspace $N \subseteq (R^3 \times R^2)$ spanned by the outward normals to the limit surface. However, since in the case under consideration the limit domain Eqs. (3) is bounded in all directions in stress space, any strain rate is normal to its boundary at some point and no constraints are introduced (i.e., $N \equiv (R^3 \times R^2)$).

Let $(\boldsymbol{\sigma}_{(\dot{\varepsilon})}, \boldsymbol{\tau}_{(\dot{\gamma})})$ denote the stress point on the limit surface associated to any given strain rate $(\dot{\boldsymbol{\varepsilon}}, \dot{\boldsymbol{\gamma}})$ through the plasticity condition. The specific dissipation power $\hat{D}(\dot{\boldsymbol{\varepsilon}}, \dot{\boldsymbol{\gamma}}) = \boldsymbol{\sigma}^t_{(\dot{\varepsilon})} \dot{\boldsymbol{\varepsilon}} + \boldsymbol{\tau}^t_{(\dot{\gamma})} \dot{\boldsymbol{\gamma}}$ is a uniquely defined function of strain rates. Its expression reads

$$\hat{D}(\dot{\boldsymbol{\varepsilon}}, \dot{\boldsymbol{\gamma}}) = \sigma_0 \sqrt{\dot{\boldsymbol{\varepsilon}}^t \boldsymbol{\Gamma}_m \dot{\boldsymbol{\varepsilon}} + \dot{\boldsymbol{\gamma}}^t \boldsymbol{\Gamma}_s \dot{\boldsymbol{\gamma}}} \tag{5a}$$

with

$$\boldsymbol{\Gamma}_m = \boldsymbol{P}_m^{-1} = \frac{1}{3}\begin{bmatrix} 4 & 2 & 0 \\ 2 & 4 & 0 \\ 0 & 0 & 1 \end{bmatrix} \qquad \boldsymbol{\Gamma}_s = \boldsymbol{P}_s^{-1} = \frac{1}{3}\begin{bmatrix} 1 & 0 \\ 0 & 1 \end{bmatrix} \tag{5b, c}$$

Eqs. (5) are obtained by specializing the general form for von Mises' materials (for its construction see, e.g., Lubliner 1990) to the case under consideration. By introducing Eq. (1a), one writes

$$\hat{D}(\dot{\boldsymbol{\kappa}}, \dot{\boldsymbol{\gamma}}) = \sigma_0 \sqrt{z^2 c_m + c_s} \qquad c_m = \dot{\boldsymbol{\kappa}}^t \boldsymbol{\Gamma}_m \dot{\boldsymbol{\kappa}} \qquad c_s = \dot{\boldsymbol{\gamma}}^t \boldsymbol{\Gamma}_s \dot{\boldsymbol{\gamma}} \tag{6a-c}$$

The dissipation power per unit plate area and for the entire plate are expressed as

$$D'(\dot{\boldsymbol{\kappa}}, \dot{\boldsymbol{\gamma}}) = \int_{-h/2}^{h/2} \hat{D}\, dz \qquad D(\dot{\boldsymbol{\kappa}}, \dot{\boldsymbol{\gamma}}) = \int_{\Omega} D'\, dx \tag{7a,b}$$

Surface and boundary loads are denoted as $\alpha p(x, y)$ and $\alpha \boldsymbol{p}_\Gamma = \alpha \{V\ W\}^t$, respectively, indicating that they are defined as a magnification through a *load multiplier* α of basic values p and $\boldsymbol{p}_\Gamma$. Then, the kinematic theorem of limit analysis states that the limit value s of α (*collapse multiplier*) is the optimal value of the minimum problem

$$s = \min_{\dot{w}, \dot{\boldsymbol{\theta}}} D(\dot{\boldsymbol{\kappa}}, \dot{\boldsymbol{\gamma}}) \tag{8a}$$

subject to

$$\dot{\boldsymbol{\kappa}} = -\nabla_s \dot{\boldsymbol{\theta}} \qquad \dot{\boldsymbol{\gamma}} = \nabla \dot{w} - \dot{\boldsymbol{\theta}} \tag{8b}$$

$$\Pi(\dot{w}, \dot{\theta}) = \int_{\Omega} p\dot{w} dx + \int_{\partial\Omega_\sigma} \boldsymbol{p}_\Gamma^t \begin{Bmatrix} \dot{w} \\ \dot{\boldsymbol{\theta}} \end{Bmatrix} dx = 1 \tag{8c}$$

along with the boundary conditions on $\partial\Omega_u$.

Eqs. (8) bring the computation of the collapse multiplier to the search of the minimum of a convex but not everywhere differentiable functional. In fact Eq. (5a) shows that the power of dissipation is a positively homogeneous function of degree one in the strain rates, not differentiable at strain rate zero. It follows that the functional to be minimized is differentiable in the region Ω_p where plastic flow develops, but not so in the remaining portion Ω_r of the plate, which keeps rigid in the mechanism, and the minimum does not correspond to a stationary point.

For simplicity, in the sequel use will be made of the compact notation

$$\tilde{\dot{\boldsymbol{\varepsilon}}}_c = \begin{Bmatrix} -\nabla_s \dot{\boldsymbol{\theta}} \\ \nabla \dot{w} - \dot{\boldsymbol{\theta}} \end{Bmatrix} \qquad \tilde{\dot{\boldsymbol{\varepsilon}}} = \begin{Bmatrix} \dot{\boldsymbol{\kappa}} \\ \dot{\boldsymbol{\gamma}} \end{Bmatrix} \qquad \tilde{\boldsymbol{\sigma}} = \begin{Bmatrix} \boldsymbol{m} \\ \boldsymbol{t} \end{Bmatrix} \qquad \boldsymbol{\Gamma} = \begin{bmatrix} z^2 \boldsymbol{\Gamma}_m & 0 \\ 0 & \boldsymbol{\Gamma}_s \end{bmatrix} \tag{9a-d}$$

where vector $\tilde{\boldsymbol{\sigma}}$ collects the static quantities conjugate, in the virtual work sense, to $\tilde{\dot{\boldsymbol{\varepsilon}}}$. In particular, $\boldsymbol{m}$ is the (bending and twisting) moment tensor and $\boldsymbol{t}$ the vector of transverse shears. Then, the Lagrangean functional of problem (8) can be written as

$$L = \int_{\Omega} \{D(\tilde{\dot{\boldsymbol{\varepsilon}}}) - \tilde{\boldsymbol{\sigma}}^t (\tilde{\dot{\boldsymbol{\varepsilon}}} - \tilde{\dot{\boldsymbol{\varepsilon}}}_c)\} dx + \alpha\{\Pi(\dot{w}, \dot{\boldsymbol{\theta}}) - 1\} \tag{10a}$$

and the optimality condition reads

$$\delta L \geq 0 \tag{10b}$$

for all variations complying with the boundary conditions on $\partial\Omega_u$. By following the same path of reasoning as in Capsoni and Corradi (1997), it can be proved that, at solution, the Lagrangean multiplier α is a load multiplier which is statically admissible and is numerically equal to the optimal value of the problem Eqs. (10). Eqs. (10) can be regarded as an alternative statement of the kinematic theorem of limit analysis.

If Kirchhoff hypothesis applies, zero transverse shear strains are assumed ($\boldsymbol{\theta}=\nabla w$) and all the preceeding relations simplify accordingly.

3. Finite element modelling and outline of the solution procedure

A discrete form of the problem can be obtained via finite element discretization. In each element e (e=1, ···, N) transverse velocities, rotation rates and associated compatible strain rates are expressed as

$$\begin{Bmatrix} \dot{w}_e(\boldsymbol{x}) \\ \dot{\boldsymbol{\theta}}_e(\boldsymbol{x}) \end{Bmatrix} = \boldsymbol{N}_e(\boldsymbol{x}) \dot{\boldsymbol{U}}_e, \qquad \tilde{\dot{\boldsymbol{\varepsilon}}}_{ce}(\boldsymbol{x}) = \boldsymbol{B}_e(\boldsymbol{x}) \dot{\boldsymbol{U}}_e \tag{11a, b}$$

where $\dot{\boldsymbol{U}}_e$ collects the nodal values for the isolated element, $\boldsymbol{N}_e(\boldsymbol{x})$ is the shape function matrix,

from which $\boldsymbol{B}_e(\boldsymbol{x})$ follows. The assemblage operation is written symbolically as

$$\dot{\boldsymbol{U}}_e = \boldsymbol{L}_e \dot{\boldsymbol{U}} \qquad (e = 1, \cdots, N) \tag{11c}$$

where $\boldsymbol{L}_e$ are suitable connectivity matrices and $\dot{\boldsymbol{U}}$ is the vector of the free parameters, i.e., assemblage is meant to enforce both interelement continuity and displacement boundary conditions.

At the element level, rigid body motions can be separated from straining modes by replacing Eq. (11b) with the two relations (Argyris 1966)

$$\tilde{\dot{\boldsymbol{\varepsilon}}}_{ce}(\boldsymbol{x}) = \boldsymbol{b}_e(\boldsymbol{x})\,\dot{\boldsymbol{q}}_e, \qquad \dot{\boldsymbol{q}}_e = \boldsymbol{c}_e \dot{\boldsymbol{U}}_e = \boldsymbol{C}_e \dot{\boldsymbol{U}} \tag{12a, b}$$

where $\dot{\boldsymbol{q}}_e$ is the vector of generalized (or *natural*) strain rates and $\boldsymbol{C}_e = \boldsymbol{c}_e \boldsymbol{L}_e$ are constant matrices, playing the role of compatibility operators for the finite elements.

As is well known, a displacement formulation of Mindlin's plate problem exhibits locking at the thin plate limit (Hughes 1987). To overcome this detrimental aspect, a mixed approach based on the variational inequality Eqs. (10) is now introduced. This requires the definition of independent models for additional fields, namely

$$\tilde{\boldsymbol{\sigma}}(\boldsymbol{x}) = \boldsymbol{S}_e(\boldsymbol{x})\,\boldsymbol{Q}_e, \qquad \tilde{\dot{\boldsymbol{\varepsilon}}}(\boldsymbol{x}) = \bar{\boldsymbol{b}}_e(\boldsymbol{x})\,\dot{\bar{\boldsymbol{q}}}_e \tag{13a, b}$$

The stress model $\boldsymbol{S}_e(\boldsymbol{x})$ is chosen so that the free parameters $\boldsymbol{Q}_e$ are the generalized stresses conjugate to $\dot{\boldsymbol{q}}_e$ according to Prager's definition (i.e., the scalar product $\boldsymbol{Q}_e^t \dot{\boldsymbol{q}}_e$ provides the integral over the finite element volume of the dissipation power). This requires that the following condition holds

$$\int_{\Omega_e} \boldsymbol{S}_e^t(\boldsymbol{x})\,\boldsymbol{b}_e(\boldsymbol{x})\,d\boldsymbol{x} = \boldsymbol{I} \tag{14}$$

If $\dim(\dot{\bar{\boldsymbol{q}}}_e) = \dim(\dot{\boldsymbol{q}}_e)$ and matrix $\bar{\boldsymbol{b}}_e(\boldsymbol{x})$ also fulfills the biorthogonality condition Eq. (14), the free parameters governing the strain model Eq. (13b) identify with the generalized strains dictated by the displacement approximation ($\dot{\bar{\boldsymbol{q}}}_e = \dot{\boldsymbol{q}}_e$, Corradi 1983) and the weak compatibility condition

$$\int_{\Omega_e} \tilde{\boldsymbol{\sigma}}_e^t (\tilde{\dot{\boldsymbol{\varepsilon}}}_{ce} - \tilde{\dot{\boldsymbol{\varepsilon}}}_e)\,d\boldsymbol{x} = 0 \tag{15}$$

is a-priori satisfied within each element, dropping out from the variational statement. In the problem at hand, stress recovery is not required and the stress model Eq. (13a) does not have to be constructed, provided that it can be proved that one of such models exists fulfilling Eq. (14) with both $\boldsymbol{b}_e(\boldsymbol{x})$ and $\bar{\boldsymbol{b}}_e(\boldsymbol{x})$. By substituting the trial functions into Eq. (10a), the discretized form of the functional reads

$$L = \sum_{e=1}^{N} D_e(\dot{\boldsymbol{U}}) - \alpha\{\boldsymbol{F}^t \dot{\boldsymbol{U}} - 1\} \tag{16a}$$

where

$$D_e(\dot{\boldsymbol{U}}) = \int_{\Omega_e} \{\int_{-h/2}^{h/2} \sigma_0 \sqrt{\dot{\boldsymbol{U}}^t \boldsymbol{\Lambda}_e(\boldsymbol{x}, z)\,\dot{\boldsymbol{U}}}\,dz\}\,d\boldsymbol{x} \tag{16b}$$

with $\boldsymbol{F}$ denoting the vector of nodal forces equivalent to basic loads and $\boldsymbol{\Lambda}(\boldsymbol{x}, z) = \boldsymbol{C}_e^t \bar{\boldsymbol{b}}_e^t(\boldsymbol{x}) \boldsymbol{\Gamma}(z) \bar{\boldsymbol{b}}_e(\boldsymbol{x})\,\boldsymbol{C}_e$. The collapse multiplier is obtained as the solution of the problem

$$\delta L \geq 0 \qquad \forall\ \delta\dot{U},\ \delta\alpha \tag{17}$$

The inequality in Eq. (17) reflects the non-stationary nature of the optimal value. In fact, due to the homogeneous of degree one character of the integrant in Eq. (16b), L is not differentiable in the regions which do not undergo plastic flow. To this purpose, it must be observed that D_e is a global value, referring to a finite element as a whole. In each element, D_e is either positive and differentiable (when $\dot{\boldsymbol{q}}_e=\boldsymbol{C}_e\dot{\boldsymbol{U}}\neq\boldsymbol{0}$) or equal to zero and not differentiable (if $\dot{\boldsymbol{q}}_e=\boldsymbol{0}$). It follows that the partitioning of Ω in the two subdomains Ω_p and Ω_r is now replaced by the partition of the set E of the N finite elements into the two subsets E_p of the $p\leq N$ plastic elements and E_r of the N-p rigid ones. This plays a key role in the solution strategy, which is now briefly outlined, referring to Capsoni and Corradi (1997) for details.

Suppose first that all elements undergo plastic flow, so that differentiability is ensured everywhere and L is stationary at solution. Then, the optimality condition reads

$$\frac{\partial L}{\partial \dot{U}}=\sum_{e=1}^{N}\left(\int_{\Omega_e}\int_{-h/2}^{h/2}\sigma_0\frac{\boldsymbol{\Lambda}_e(x,z)}{\sqrt{\dot{\boldsymbol{U}}^t\boldsymbol{\Lambda}_e(x,z)\dot{\boldsymbol{U}}}}\,dxdz\right)\dot{\boldsymbol{U}}-\alpha\boldsymbol{F}=\boldsymbol{0} \tag{18}$$

Eq. (18) can be solved by direct iteration through the following steps

$$\boldsymbol{H}_j=\sum_{e=1}^{N}\left(\int_{\Omega_e}\int_{-h/2}^{h/2}\sigma_0\frac{\boldsymbol{\Lambda}_e(x,z)}{\sqrt{\dot{\boldsymbol{U}}_j^t\boldsymbol{\Lambda}_e(x,z)\dot{\boldsymbol{U}}_j}}\,dxdz\right) \tag{19a}$$

$$\dot{\boldsymbol{U}}_*=\boldsymbol{H}_j^{-1}\boldsymbol{F},\qquad \alpha_j=\frac{1}{\boldsymbol{F}^t\dot{\boldsymbol{U}}_*},\qquad \dot{\boldsymbol{U}}_{j+1}=\alpha_j\dot{\boldsymbol{U}}_* \tag{19b-d}$$

Eq. (19c) provides the current estimate of the Lagrangean multiplier α in Eq. (16a). As for its continuous counterpart Eq. (10a), at solution this value is numerically equal to the optimal value of the objective function. This property establishes that solution is attained when one has, to within a given accuracy

$$\sum_{e=1}^{N}D_e(\dot{\boldsymbol{U}}_j)=\alpha_{j+1} \tag{19e}$$

As described, the procedure does not consider that often the collapse mechanism entails plastic flow in some elements only. To account for this occurrence, the procedure is started with a tentative vector $\dot{\boldsymbol{U}}_0$ defined so as to induce plastic flow in all elements. At each iterative step the dissipation power is computed separately for each element and when it gets smaller than a prescribed tolerance, the relevant element is predicted as rigid in the final mechanism. For that element, generalized strain rates must vanish and only rigid body motions survive in the sequel. Account taken of Eq. (12b), the condition reads

$$\dot{\boldsymbol{q}}_e=\boldsymbol{C}_e\dot{\boldsymbol{U}}_0=\boldsymbol{0} \tag{20}$$

Eq. (20) provides some constraints among the components of vector $\dot{\boldsymbol{U}}_0$, which can be replaced by a smaller size vector $\dot{\boldsymbol{U}}_1$ by writing $\dot{\boldsymbol{U}}_0=\boldsymbol{G}^1\dot{\boldsymbol{U}}_1$. Then, the iteration process is continued with the rigid element ignored and the operation is repeated whenever the dissipation power of a new element gets sufficiently small.

The procedure aims at identifying the finite elements which are not involved in the collapse

mechanism, gradually transferring them from the set E_p of plastic elements (initially including all elements) to the (initially empty) set E_r of rigid ones. A sequence of systems with a progressively decreasing number of elements and of free nodal parameters is thus considered. Each system consists of plastically deforming elements only, and its dissipation power must be stationary at solution.

An inherent limitation of the procedure is that an element cannot be removed from the rigid set E_r once it has been introduced in it. The structure is progressively modified by the addition of constraints and, whenever this happens, the collapse multiplier of a different structure is searched. Strictly speaking, the solution obtained should be regarded merely as a kinematically admissible value, bounding from above the collapse multiplier of the original system. However, the numerical experience gained so far seems to indicate that no wrong elements enter the rigid set.

4. Remarks on the dissipation power for solid plates

The computation of the dissipation power per unit surface, as defined by Eqs. (7a) and (6), is worth a comment. For Kirkhhoff plates, c_s=0 is assumed and one obtains

$$D'(\dot{\boldsymbol{\kappa}}) = \sigma_0 \frac{h^2}{4} \sqrt{c_m} = m_0 \sqrt{\dot{\boldsymbol{\kappa}}^t \boldsymbol{\Gamma}_m \dot{\boldsymbol{\kappa}}} \tag{21a}$$

where $m_0=\sigma_0 h^2/4$ is the fully plastic moment for solid plates. When shear deformations are accounted for, the expression of D' reads

$$D'(\dot{\boldsymbol{\kappa}}, \dot{\boldsymbol{\gamma}}) = \int_{-h/2}^{h/2} \hat{D}\, dz = \frac{\sigma_0 h}{2} \sqrt{c_s + \frac{h^2}{4} c_m} - \frac{\sigma_0 c_s}{2\sqrt{c_m}} \ln \left(\frac{\sqrt{c_s + \frac{h^2}{4} c_m} + \frac{h\sqrt{c_m}}{2}}{\sqrt{c_s + \frac{h^2}{4} c_m} - \frac{h\sqrt{c_m}}{2}} \right) \tag{21b}$$

Such an expression is not convenient for numerical purposes because, when c_s gets small at the thin plate limit, the last term is very nearly singular and numerical integration is preferable. To avoid inaccuracies associated with the point z=0, twice the integral over half thickness is considered. Then one can write

$$D'(\dot{\boldsymbol{\kappa}}, \dot{\boldsymbol{\gamma}}) = 2 \int_0^{h/2} D(\dot{\boldsymbol{\kappa}}, \dot{\boldsymbol{\gamma}})\, dz \cong m_0 \sum_{g=1}^{G} W_g \sqrt{(1+\zeta_g)^2 c_m + \frac{16}{h^2} c_s} \tag{22}$$

where $\zeta=4z/h-1$ and ζ_g, W_g are the usual Gauss-Legendre integration point coordinates and weights. For $G \geq 5$, Eqs. (22) and (21b) give practically coincident results for all c_s/c_m ratios.

It is of interest to observe that when G=1 is used (ζ_1=0, W_1=2.0), Eq. (22) produces the expression of D' associated to the approximate yield condition

$$\Phi(\boldsymbol{m}, \boldsymbol{t}) = \sqrt{\boldsymbol{m}^t \boldsymbol{P}_m \boldsymbol{m} + \frac{3h^2}{16} \boldsymbol{t}^t \boldsymbol{P}_s \boldsymbol{t}} - m_0 \tag{23}$$

often used for Mindlin solid plates because of its simplicity (Papadopoulus and Taylor 1991). Eq. (23) extends to plates the limit domain of ideal I-beams under combined bending and shear,

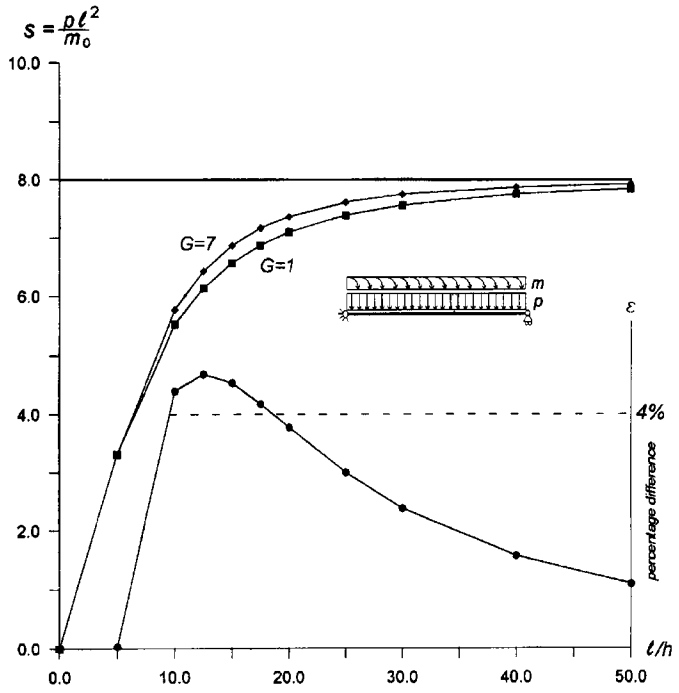

Fig. 1 Timoshenko beam solution – $m=3pl$

which is somewhat narrower than the domain for a beam of rectangular cross section. The relevant limit curve, defined only in parametric form, is cumbersome to use, which restricts any attempt at extensions to plates. However, the associated dissipation power is expressed by Eq. (21b) (Hodge 1959) and there is no need for approximations when, as in the present approach, an explicit expression for the limit domain is not required.

To assess the error associated with the use of the simplified expression, a Timoshenko beam of rectangular cross section, hinged at both ends, was examined. The beam was subject to a uniform transverse load p and to a moment distribution of intensity $m=3pl$ per unit length, inducing severe shears. The dissipation power per unit length was computed from Eq. (22) using $G=1$ (ideal I-beam approximation) and $G=7$ (*exact*) Gauss points and the resulting collapse multiplier is plotted in Fig. 1 as a function of the l/h ratio. In the interval $8 \leq l/h \leq 20$, the two solution differ by more than 4%, a discrepancy of engineering significance even if not dramatic (for short beams, failure occurs because the limiting value for shear is attained at the right end support and dissipation is exactly integrated with a single Gauss point). The maliciously chosen load condition clearly emphasizes differences, but the computation of the dissipation power for solid plates through Eq. (22) does not entail any difficulties discouraging its use.

5. Illustration and discussion of numerical examples

A few numerical solutions of rectangular plates (sides $2a \times 2b$) were computed and are now discussed. Regular meshes of square, equal elements were only employed. For Kirchhoff plates, the 4-node, 16 d.o.f. element proposed by Bogner, Fox and Schmidt (Zienkiewicz and Taylor

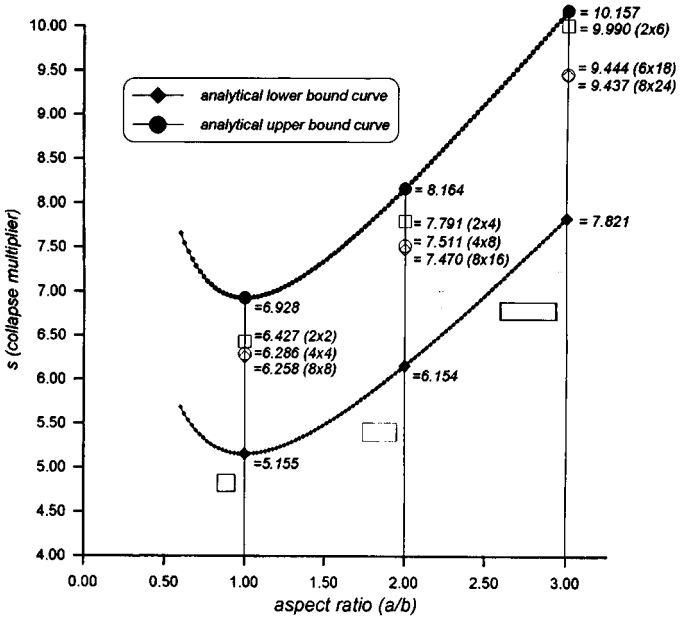

Fig. 2 Collapse multiplier for uniformely loaded, simply supported rectangular plates

1989) was adopted. The element is C^1 continuous, ensuring that compatibility is enforced throughout. Its well known sensitivity to mesh distortion does not cause inconveniencies as long as the element is mantained of rectangular shape.

Fig. 2 shows some results for simply supported rectangular plates under uniform transverse pressure as function of the aspect ratio a/b (basic load $p=m_0/ab$). Because of symmetry, only one quarter of the plate is considered. Results are compared to upper bounds derived by yield line theory and lower bounds obtained as proposed in Hodge (1959). In all cases, convergence with mesh refinement is approached already with coarse discretizations. The more stringent bounds indicated in Save (1995), when applicable, were also complied with. Fig. 3 shows the collapse mechanism predicted for $a/b=3$ (rigid elements are dashed): the picture bears similarities with the optimal yield line mechanism, but the relevant upper bound estimate was lowered by about 7%.

Square plates under uniform pressure were also analyzed with different boundary conditions. The computed collapse multipliers for the simply supported case and for plates simply supported along three edges and the forth edge free are listed in Table 1, along with the best bounds so far available, as reported by Save (1995): in both cases previous upper bounds are improved already with coarse meshes and convergence to four significant figures is rapidly achieved. Previous upper bounds are reduced by 1.4% and 6.7% respectively. For the simply supported case, the percentage difference with respect to the lower bound is a mere 0.6%, indicating that the collapse multiplier can be considered as identified for engineering purposes.

Results are not equally good in other instances. Fig. 4 shows the computed collapse multiplier for a clamped square plate under uniform pressure as function of the number of degrees of freedom (for one quarter of plate). The discretization ensuring convergence in the simply supported case (6×6 elements) now improves only slightly the upper bound established by Hodge and Belytschko (1968). The mesh was refined up to a 20×20 grid and computed values kept decreasing at a small, but slowly diminishing, rate. In any case, the difference with respect to the

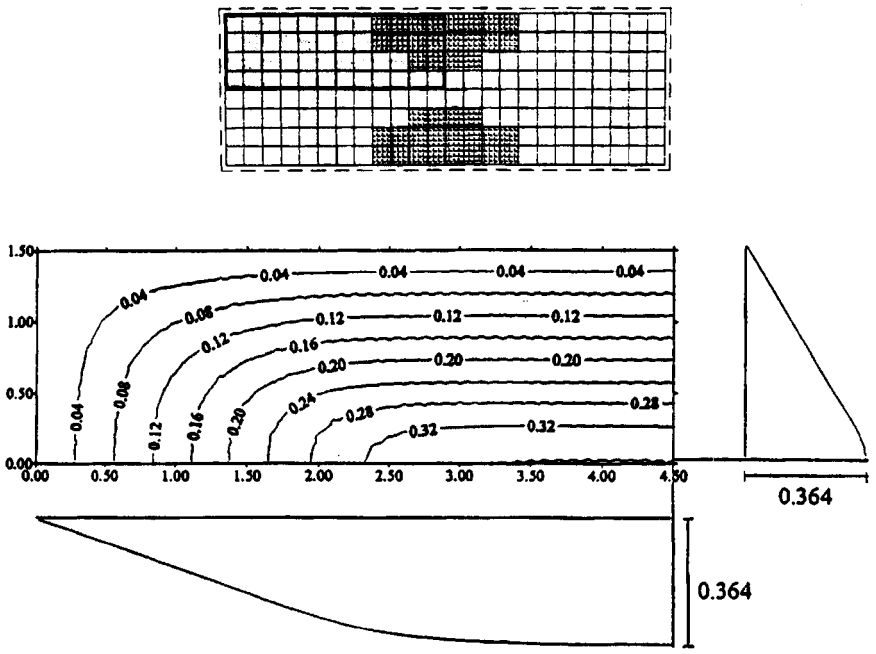

Fig. 3 Collapse mechanism for a uniformely loaded, simply supported plate – a/b=3

Table 1 Collapse multipliers for square plates under uniform pressure (basic load $p=m_0/a^2$): [a] Del Rio Cabrera (1970); [b] Hodge and Belytschko (1968)

		Simply supported	3 edges s.s. 1 free
Upper bound		6.348 [a]	3.924 [b]
Present	1	6.427	3.706
Results	2	6.286	3.669
	3	6.266	3.664
Number of	4	6.258	3.662
Elements ⇒	5	6.256	3.662
Per half side	6	6.256	
Lower bound		6.216 [b]	3.570 [b]

best lower bound known was reduced from 15% to 5.6%.

Square plates loaded by a point force at their center (basic value $P=m_0$) were also considered. Reference results are exact solutions of circular plates. For a clamped boundary, the collapse multiplier is s=7.255 (Hopkins and Wang 1954) and applies to clamped plates of any shape. This value provides an upper bound for the simply supported plate, while the best lower bound known amounts to 6.401 (Hodge and Belytschko 1968). Present results are illustrated in Fig. 5. In the simply supported case, the upper bound eventually is slightly lowered, but for the clamped plate the collapse multiplier is grossly overestimated even with the finest mesh and hardly can be expected to be approached with further refinement.

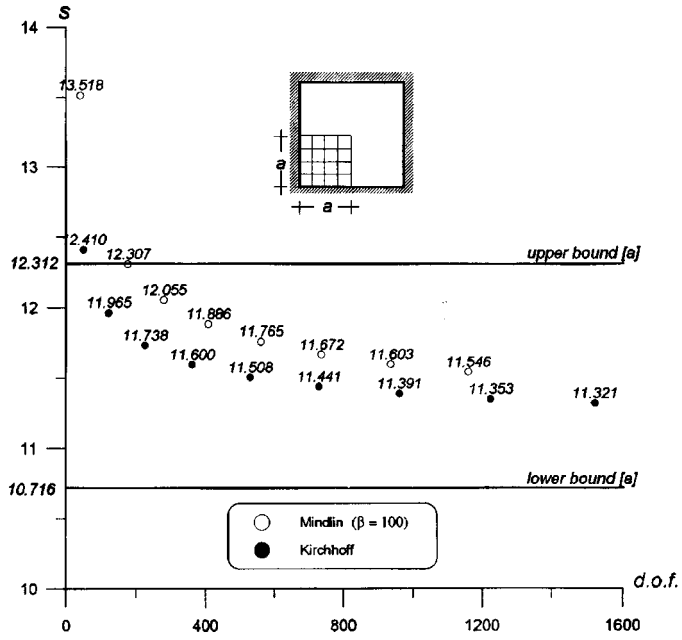

Fig. 4 Collapse multipliers for a uniformely loaded, clamped square plate. [a] Hodge and Belytschko (1968)

The discrepancy can be explained by considering the related problems of circular axisymmetric plates (radius R). If Tresca's condition is assumed the exact solution, given by Hopkins and Prager (1953), is readily computed. By supposing that a load m_0 is uniformly distributed on a circle of radius a and by letting $a \rightarrow 0$, the collapse multiplier for a point force at the center is $s=2\pi=6.283$ regardless of boundary conditions. However, while in the simply supported case this value is very nearly constant for small a, for clamped plates the collapse multiplier grows sharply, to the point that for $a=R/100$ it has already increased by a factor of 1.29, which accounts for more than the difference between computed and exact results (dashed lines in Fig. 6). For von Mises' criterion, closed form results are also available (Hopkins and Wang 1954), but are not equally easy to compute. However, the dependence of the load carrying capacity from a is analogous (solid lines in Fig. 6). The finite element model hardly can distinguish between a truly point load and one acting over a small area and numerical results are affected by the sensitivity of the problem to the actual load condition.

In spite of the considerations above, the use of finite elements did not prevent that a much better bound, only the 8% in excess of the exact value, be computed by Hodge and Belytschko (1968). The element used was C^1 discontinuous and, even if the dissipation along slope discontinuity lines was accounted for, it is likely to be more flexible than the fully compatible element used here. Apparently, this capability does not provide benefits if loads are distributed, but the velocity field near a point force, which exhibits a logarithmic singularity (Eason 1958), is poorely represented by a fully compatible model, no matter how flexible. Fig. 7 depicts the dissipation of each element in the collapse mechanism predicted for the clamped plate and a mesh of 16×16 elements. More than 22% of the total value (amounting to 9.260) is contributed by the element adjacent to the load, which the zero slope constraint at the center makes too stiff to account for local velocities correctly.

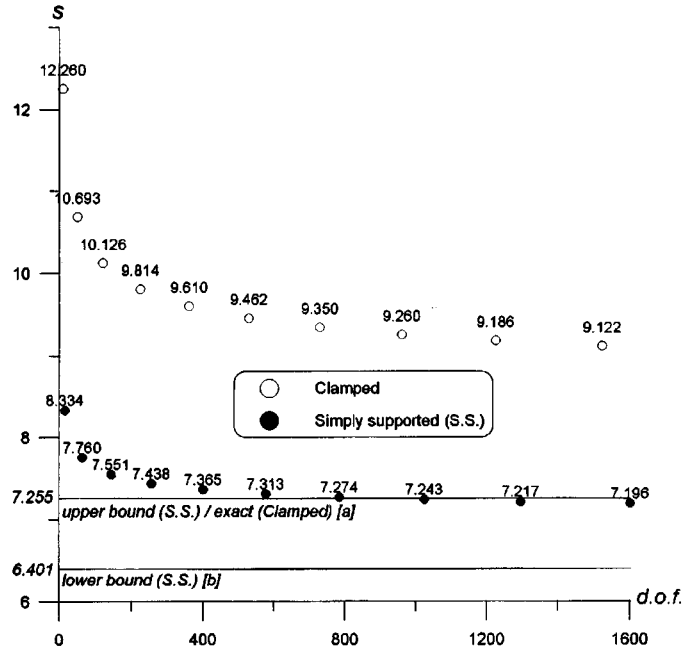

Fig. 5 Collapse multipliers for square plates under a point force: [a] Hopkins and Wang (1954); [b] Hodge and Belytschko (1968)

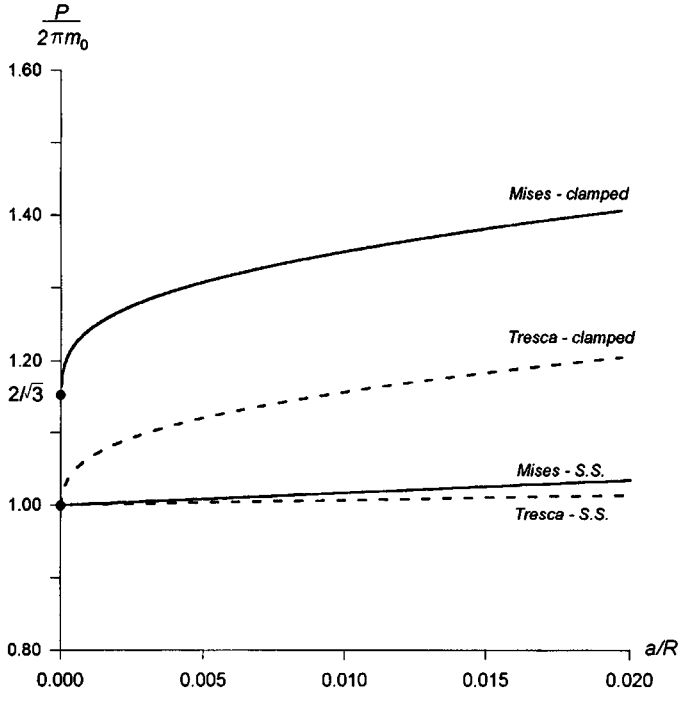

Fig. 6 Collapse multipliers for circular plates uniformely loaded on a central circle of radius a (Tresca condition: computed from formulas in Hopkins and Prager 1953; von Mises' condition: redrawn from Fig. 3 in Hopkins and Wang 1954)

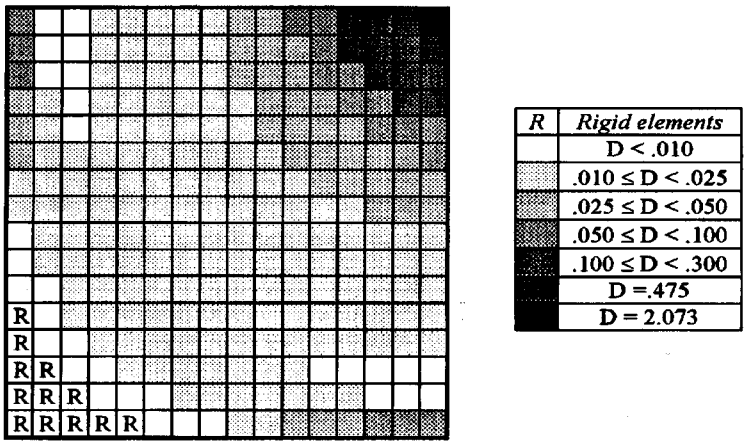

Fig. 7 Element dissipation in a clamped Kirchhoff plate under point force at its center (mesh 16×16 elements for one quarter of plate)

Mindlin plates were next considered, by employing a four-node, bilinear element. Model $\boldsymbol{b}_e(\boldsymbol{x})$, governing compatible strains is in this case

$$\boldsymbol{b}_e(\boldsymbol{x})=\begin{bmatrix} 1 & 0 & 0 & 0 & 0 & 0 & 0 & y & 0 \\ 0 & 1 & 0 & 0 & 0 & 0 & 0 & 0 & x \\ 0 & 0 & 1 & 0 & 0 & 0 & 0 & x & y \\ -x & 0 & 0 & 1 & 0 & y & 0 & -xy & 0 \\ 0 & -y & 0 & 0 & 1 & 0 & x & 0 & -xy \end{bmatrix} \tag{24a}$$

where x, y are intrinsic coordinates, ranging from -1 to 1. The independent strain model $\bar{\boldsymbol{b}}_e(\boldsymbol{x})$ was assumed as follows

$$\bar{\boldsymbol{b}}_e(\boldsymbol{x})=\begin{bmatrix} 1 & 0 & 0 & 0 & 0 & 0 & 0 & y & 0 \\ 0 & 1 & 0 & 0 & 0 & 0 & 0 & 0 & x \\ 0 & 0 & 1 & 0 & 0 & 0 & 0 & 0 & 0 \\ 0 & 0 & 0 & 1 & 0 & y & 0 & 0 & 0 \\ 0 & 0 & 0 & 0 & 1 & 0 & x & 0 & 0 \end{bmatrix} \tag{24b}$$

As comparison shows, Eq. (24b) is derived from Eq. (24a) simply by eliminating the locking inducing terms which couple transverse shear and membrane strains. Also terms coupling bending and twisting and causing parasitic strains were cancelled. The model can be shown to comply with the requirements stated in Sec. 3. In particular, the strain rate distribution within each element is governed by the generalized values $\dot{\boldsymbol{q}}_e$ dictated by the displacement approximation.

The need for a modified strain model is evident from Fig. 8, referring to a square, simply supported plate under uniform transverse load. The normalized collapse multiplier s/s_k (s_k= 6.256 being the converged Kirchhoff value) is plotted as function of the plate slenderness ratio β= $2a/h$. Two different discretizations are used, involving 16 and 64 elements for one quarter of plate,

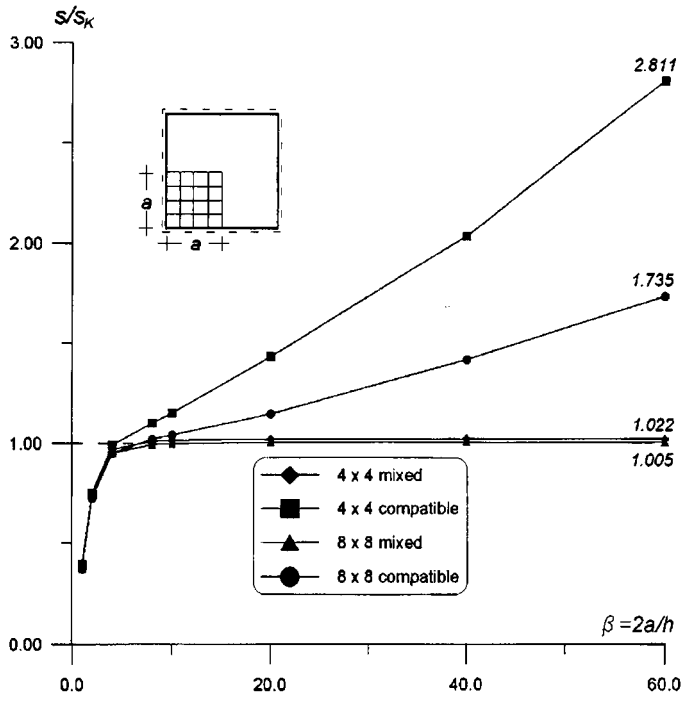

Fig. 8 Simply supported square plate under uniform pressure: collapse multiplier vs. slenderness ratio – s_k=converged Kirchhoff value

respectively. As the plate gets thin, the *compatible* solutions, obtained on the basis of the strain model Eq. (24a), exhibits locking, which is removed if Eq. (24b) is used instead (*mixed* solutions).

The figure also shows that the upper bound nature of the result is not jeopardized by the mixed character of the formulation. Actually, the Mindlin element used turns out to be stiffer than Kirchhoff's, as evidentiated by the fact that with a 8×8 mesh (more than required to reach convergence in previous analyses, see Table 1), the collapse multiplier for thin plates is still 0.5% in excess of the Kirchhoff value. The two results get closer with further mesh refinement, as shown in Fig. 9, where the percentage difference with respect to the converged Kirchhoff value is plotted versus the number of degrees of freedom for the two cases in Table 1 (β=100 was considered, i.e., plates thin enough to make transverse shear strain effects negligible). When convergence is slow even in the Kirchhoff case, the additional stiffness of the Mindlin element is detrimental. For a clamped plate, the two solutions are compared in Fig. 4 and it appears that Mindlin's model requires more than twice as many degrees of freedom to produce comparable results. Obviously, Mindlin's formulation does not apply to point loads, since the singularity in shears would make the collapse multiplier vanish.

In any case, the Mindlin approach permits the assessment of the influence of transverse shear deformations on the collapse multiplier of thick plates. Fig. 10 shows, as function of the plate slenderness β, the ratio $s(\beta)/s(\beta=100)$ for uniformly loaded square plates either simply supported or clamped along their boundaries. For β=10, the difference is already nearly negligible in the first case, while in the second one a 7% decay is predicted. The decay is still of 1.7% for β=20, i.e., for a plate not unreasonably thick. It is worth mentioning that the above ratio is influenced little if at all by the mesh used and, hence, by the accuracy of the result at the thin plate limit. Therefore,

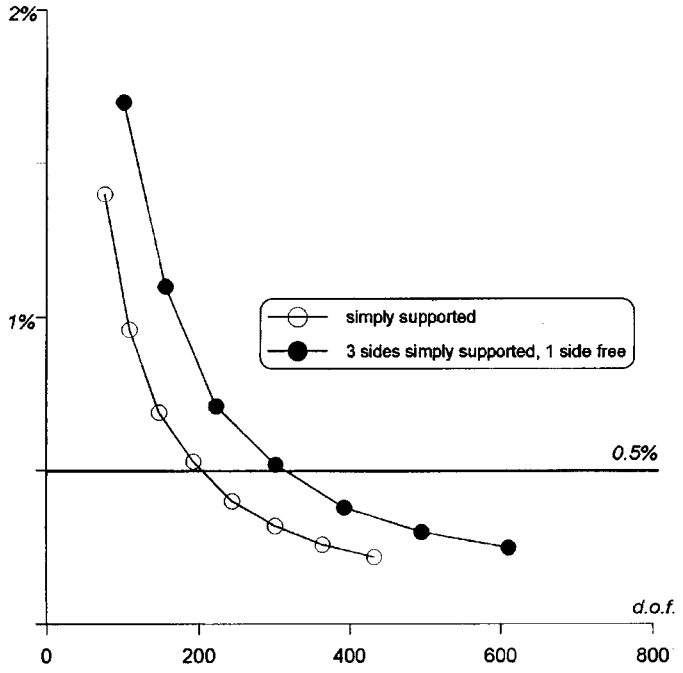

Fig. 9 Percentage difference of Mindlin plate solution (β=100) with respect to converged Kirchhoff value

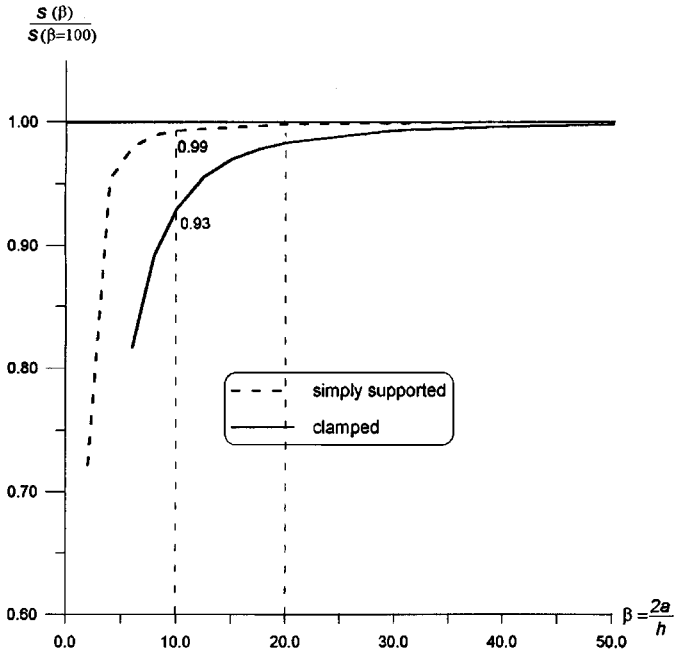

Fig. 10 Influence of slenderness ratio on the collapse multiplier of uniformely loaded square plates

it can be applied to the relevant Kirchhoff plate solution to measure the influence of transverse shear.

6. Conclusions

The procedure proposed in this paper appears capable of producing good upper bounds to the collapse load of plates in bending, as witnessed by the fact that existing results were improved in all but one, in a sense pathological, case. In some instances, convergence with mesh refinement is rapidly achieved and when, as for the situations listed in Table 1, it is obtained with both Kirchhoff and Mindlin formulations, converged results coincide for practical purposes. Even if lacking the support of a statically admissible solution, this suggests that the correct value of the collapse multiplier was maybe identified.

The finite elements used do not allow for slope discontinuities. Apparently, this does not compromise the convergence capability of the model, even if convergence may get slow when the collapse mechanism implies strong curvature gradients. The only exception is the case of a clamped plate loaded by a point force at its center, when the known exact collapse multiplier is far from being approached. However, as discussed, the problem is extremely sensitive to the actual load condition, in that the collapse load value increases sharply if the force is distributed over an even extremely small area, which makes this case a test only partially meaningful. In any case, the possibility of including slope discontinuities, accounting for dissipation along discontinuity lines so as to preserve the upper bound nature of the approach, might improve the performance of the model when convergence is slow and it is worth exploring within the present context.

A final comment refers to the kinematic character of the discrete models, which assess the upper bound nature of computed results. The Kirchhoff plate, fully compatible element used certainly meets this requirement, but when dealing with Mindlin's formulation compatibility is relaxed to avoid locking. It was stated previously that the conditions indicated in Sec. 3, namely that the strain distribution within each element is governed by the same parameters dictated by the displacement approximation and that the biorthogonality condition Eq. (14) is complied with by the strain model as well, preserve the kinematic nature of the discrete scheme. This is a conjecture one of the authors has made a few years since (Corradi 1983) and which was always corroborated by the numerical experience gained also in different contexts (e.g., plane strain situations), but attempts to produce a formal proof so far have failed. In any case, the performances of the Mindlin plate element employed seem to confirm it.

The upper bound nature of the results could, in principle, also be compromised by the approximations connected with the computation of the dissipation power by means of numerical integration. The results above were obtained with Gauss-Legendre integration over a 3×3 grid on the element area and, for Mindlin plates, with G=3 integration points over half thickness. A few computations performed with more refined formulas indicate that the numerical integration error does not affect the results to within four significant figures.

Acknowledgements

This research was supported by the Italian Ministry of University and Scientific and Technological Research (*M.U.R.S.T.*). Authors acknowledge with thanks the contribution of A. Ravasi, F. Scalvini, P. Scorza and A. Vecchi, who performed some of the computations as a part of their graduation theses at the *Politecnico di Milano*.

References

Argyris, J.H. (1966), "Continua and discontinua", *Proc. 1st Conf. Matrix Methods in Structural Mechanics*, AFFDL, TR 66-88, Dayton OH, 11-92.

Bottero, A., Negre, R., Pastor, J. and Turgeman, S. (1980), "Finite element method and limit analysis theory for soil mechanics problems", *Comp. Meth. Appl. Mechns Engng.*, **22**, 131-149.

Capsoni, A. and Corradi, L. (1997), "A finite element formulation of the rigid-plastic limit analysis problem", *Int. J. Num. Methods Engng.*, **40**, 2063-2086.

Casciaro, R. and Cascini, L. (1982), "A mixed formulation and mixed finite elements for limit analysis", *Int. J. Num. Methods Engng.*, **18**, 211-243.

Cohn, M.Z. and Maier, G., edts. (1979), *Engineering Plasticity by Mathematical Programming*, Pergamon Press, New York, NY.

Corradi, L. (1983), "A displacement formulation for the finite element elastic-plastic problem", *Meccanica*, **18**, 77-91.

Christiansen, E. and Larsen, S. (1983), "Computations in limit analysis for plastic plates", *Int. J. Num. Methods Engng.*, **19**, 169-184.

Del Rio Cabrera, L. (1970), *Limit Analysis of Rectangular Plates* (in French), Master thesis, Mons, Belgium.

Eason, G. (1958), "Velocity fields for circular plates with the von Mises yield condition", *J. Mech. and Phys. Solids*, **6**, 231-235.

Hodge, Ph. G. Jr (1959), *Plastic Analysis of Structures*, McGraw-Hill, New York, NY.

Hodge, Ph. G. Jr and Belytschko, T. (1968), "Numerical methods for the limit analysis of plates", *Trans. ASME, J. Appl. Mech.*, **35**, 796-802.

Hopkins, H.G. and Prager, W. (1953), "The load carrying capacity of circular plates", *J. Mech. and Phys. Solids*, **2**, 1-13.

Hopkins, H.G. and Wang, A.J. (1954), "Load carrying capacity for circular plates of perfectly-plastic material with arbitrary yield condition", *J. Mech. and Phys. Solids*, **3**, 117-129.

Hughes, T.J.R. (1987), *The Finite Element Method*, Prentice-Hall, New York, NY.

Jiang, G.L. (1995), "Nonlinear finite element formulation of kinematic limit analysis", *Int. J. Num. Methods Engng.*, **38**, 2775-2807.

Liu, Y.H., Cen, Z.Z. and Xu, B.J. (1995), "A numerical method for plastic limit analysis of 3-D structures", *Int. J. Solids Struct.*, **32**, 1645-1658.

Lubliner, J. (1990), *Plasticity Theory*, Macmillan, New York, NY.

Papadopoulus, P. and Taylor, R.L. (1991), "An analysis of inelastic Reissner-Mindlin plates", *Finite Elements in Analysis and Design*, **10**, 221-233.

Ponter, A.R.S. and Carter, K.F. (1997), "Limit state solutions based upon linear elastic solutions with a spatially varying elastic modulus", *Comp. Meth. Appl. Mechns Engng.*, **140**, 237-258.

Save, M. (1995), *Atlas of Limit Loads of Metal Plates, Shells and Disks*, Elsevier, Amsterdam.

Sloan, S.W. and Kleeman, P.W. (1995), "Upper bound limit analysis using discontinuous velocity fields", *Comp. Meth. Appl. Mechns Engng.*, **127**, 293-314.

Yang, G. (1988), "Panpenalty finite element programming for plastic limit analysis", *Comput. Struct.*, **28**, 749-755.

Zienkiewicz, O.C. and Taylor, R.L. (1989), *The Finite Element Method*, **2**, McGraw-Hill, London, U.K.